

Storage and Retrieval of an Image using Four-Wave Mixing in a Cold Atomic Ensemble

Jinghui Wu[†], Dongsheng Ding, Yang Liu, Zhiyuan Zhou, Baosen Shi^{††}, Xubo Zou, and Guangcan Guo
Key Laboratory of Quantum Information, Chinese Academy of Sciences, University of Science and Technology of China, Hefei, P. R. China, 230026

We experimentally realized storage and retrieval of an image of light in a cold atomic ensemble in a two-dimensional magneto-optical trap of Rubidium 85 using four-wave mixing (FWM) for the first time. The input signal and the generated idler beams in the FWM process, both carrying images, can be simultaneously mapped into and out of the long-lived ground state coherence of the atoms. We also observed the oscillations of the retrieval efficiencies of signal and idler due to the time evolution of the ground state coherence of atoms in a uniform magnetic field, which is an exhibition of the storage of phases of signal and idler. This image storage technique holds promise for application in image processing, remote sensing and quantum communication.

PACS number(s): 03.67.-a, 32.80.Qk, 42.30.-d

[†]e-mail: wjh1987@mail.ustc.edu.cn

^{††}Corresponding author: drshi@ustc.edu.cn

In the field of quantum communication, a quantum memory in which photons are stored in and then retrieved from a medium with a high efficiency is required [1]. A lot of progresses have been made in the candidate systems of quantum memories, such as cold atoms in magneto-optical trap (MOT) [2], warm atoms in vapor cells [3], Bose-Einstein condensate [4], rare-earth-doped crystals at low temperatures [5], *etc.* Usually, one-dimensional optical information is stored, such as light pulses with a uniform spatial profile (*i.e.*, no spatial information) and variation temporally only. However, the research interests have been recently extended to high-dimensional information storage (specially the spatial information), such as orbital angular momentum [6-7], transverse momentum and position [8], multiple transverse modes [9-14], *etc.* The spatial information has always been a communication medium choice because of the large amount of information they can carry. A high-dimensional state shows many interesting properties compared with a one-dimensional state.

The technique of electromagnetically induced transparency (EIT) [15, 16] was successfully applied in quantum memory in a variety of systems (solid, gas, *etc.*). EIT can be used to make a resonant, opaque medium transparent by means of quantum interference. Meanwhile, the optical properties of the medium will be dramatically modified, *e.g.* great enhancement of nonlinear susceptibility in the spectral region of induced

transparency and associated steep dispersion. The steep dispersion is necessary to realize light-slowing and -storage. In typical storage experiments, spatially compressing the pulse in medium is primary. Then the information in the light (frequency, amplitude, phase and spatial mode, *etc.*) is mapped into long-lived atomic coherence by adiabatically switching off the control light. Sometime later, the coherence can be read out into electromagnetic field by turning the control light back on. This process can be understood in terms of a quasi-bosonic particle, a so-called dark-state polariton (DSP) [17, 18]. The enhanced nonlinear susceptibility is useful in frequency mixing process, such as four-wave mixing (FWM) [19]. Combining the EIT and FWM, the storage of light using FWM have been studied [20] in hot atomic rubidium vapor, where the input signal and the generated idler can be simultaneously stored by adiabatically switching off the pump laser. The phase coherence between the retrieved signal and idler recently has been demonstrated experimentally [21] by obtaining the beating between them. This kind of storage will improve the fidelity of storage technique for practical usage [22] and two coherent fields can be stored. So far, there is no any report on the storage and retrieval of an image using FWM. This image storage may have important implications in image processing, remote sensing and quantum communication, where two correlated fields need to be preserved for later use.

In this paper, we report on the first experimental storage and retrieval of an image using a FWM process based on a two-dimensional MOT [23]. Instead of storing the image itself, we mapped the Fourier transform of the image [12, 14] into the atomic ensemble. This improvement can further reduce the diffusion of the atoms and dramatically enhance the stability of the storage process [12] though we have got the atoms with low enough temperature (about 100 μ K). Besides, the usage of non-collinear backward-wave FWM geometry can significantly decrease the noises from the pump laser. Finally, due to the Larmor precession of the ground state coherence of the atoms in an applied uniform magnetic field, the oscillations of retrieval efficiencies of signal and idler have been observed [24]. The oscillations are synchronous, which can be regarded as a proof of storing phase coherence between signal and idler beams.

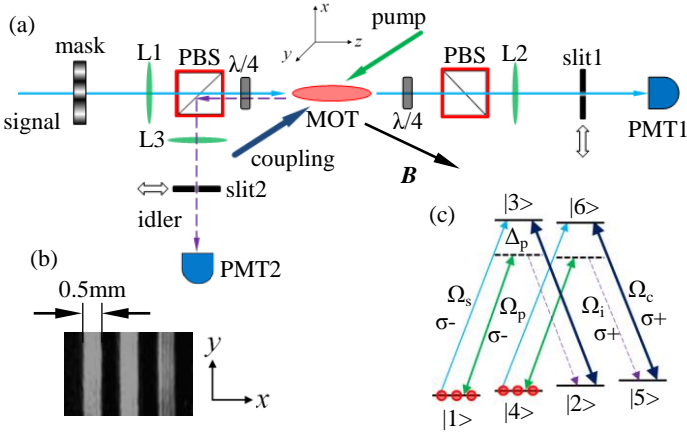


FIG. 1. (a) Experimental setup. All the experimental laser beams come from one external-cavity diode laser (DL100, Toptica). Their frequencies are modulated by some acousto-optic modulators. The $1/e^2$ beam diameter of signal is approximately 5mm at the object plane and those of coupling and pump approximately 3.6mm and 3.2mm respectively. The peak powers of signal, coupling and pump are approximately 200pW, 200 μ W and 3.6mW respectively. Here, PBS is polarizing beam splitter; $\lambda/4$, quarter-wave plate; PMT, photomultiplier tube (Hamamatsu, H10721); mask (1951 USAF resolution target). The transparent windows of slit1 and slit2 are aligned in the y-axis. (b) When we put a CCD camera in the position of slit1, the picture of cw signal imprinted with image is captured. (c) The D_1 transition of ^{85}Rb creates a double- Λ configuration. Coupling is resonantly connected to transition $|2\rangle$ ($5^2S_{1/2}$, $F=3$, $m_F=-1$) \rightarrow $|3\rangle$ ($5^2P_{1/2}$, $F=2$, $m_F=-2$), and signal is to state $|1\rangle$ ($5^2S_{1/2}$, $F=3$, $m_F=-3$) to state $|3\rangle$. The pump is detuned by 80MHz to the red of the optical transition connecting $|1\rangle$ and $|3\rangle$.

The experimental setup is illustrated in Fig. 1(a). The atoms are obtained from a two-dimensional MOT [23] and the cigar-like atomic cloud is aligned in the z-axis

(see, Fig. 1(a)). Three pairs of Helmholtz coils (not shown) are used to generate a uniform magnetic field B (Fig. 1(a)) in the center of the atomic cloud. Input signal, coupling, pump and generated idler form an off-axis backward-wave FWM configuration [19]. All beams are in the x-z plane. Coupling and pump are collimated and coupled with each other. Signal comes out from a collimated fiber, then passes through a mask, and at last is focused to the center of atomic cloud (transform plane) by lens L1 in the z-axis, which makes the optical depth of the cloud largest. Coupling and pump totally overlap signal in the atomic cloud. We put the mask in the front focal plane of lens L1 (*i.e.* object plane). The front focal plane of lens L2 is coincident with the back focal plane of lens L1 in the transform plane. Hence, the object plane, lens L1, transform plane, lens L2 and image plane (the back focal plane of lens L2, where we will put CCD camera or slit1) compose a $4f$ imaging system. Because of the phase-matching condition in FWM process, the absolute value of the divergence of idler field is the same as that of the convergence of signal field. That means, another $4f$ imaging system consists of the object plane, lens L1, transform plane, lens L3 and slit2 (the back focal plane of lens L3). The image of signal after the $4f$ system is showed in Fig. 1(b). The angle between the signal-idler axis and coupling-pump axis is 1.5° .

For the experiment, we used the Zeeman sublevels of the degenerate two-level system associated with the D_1 transition of ^{85}Rb atoms ($5^2S_{1/2}$, $F=3 \rightarrow 5^2P_{1/2}$, $F=2$) (Fig. 1(c)). The repetition of the experiment is 34Hz. During each experimental period, the atoms are loaded for 29.2ms and the experimental window is 200 μ s. The cooling beams and Ioffe coils are shuttered off during the experiment. The repumper is always on to keep the atoms in the state $|5^2S_{1/2}$, $F=3\rangle$. Coupling laser resonantly couples the transition $5^2S_{1/2}$, $F=3 \rightarrow 5^2P_{1/2}$, $F=2$ with $\sigma+$ polarization and signal with $\sigma-$ polarization. The strong coupling and weak signal form a generic Λ -type EIT configuration. The strong pump is $\sigma-$ polarized and set to the red detuning (80MHz) of D_1 transition. These three lasers compose a double- Λ FWM level system. The coupling and the pump are switched on before signal laser by $\sim 20\mu$ s for the preparation of initial states. Hence, the atoms are appropriately pumped into the states $5^2S_{1/2}$, $F=3$, $m_F=-3$ and $m_F=-2$. Therefore, there are two independent FWM cycles (shown in Fig. 1(c)). Because of the independence of these two cycles, we will take one cycle into account below.

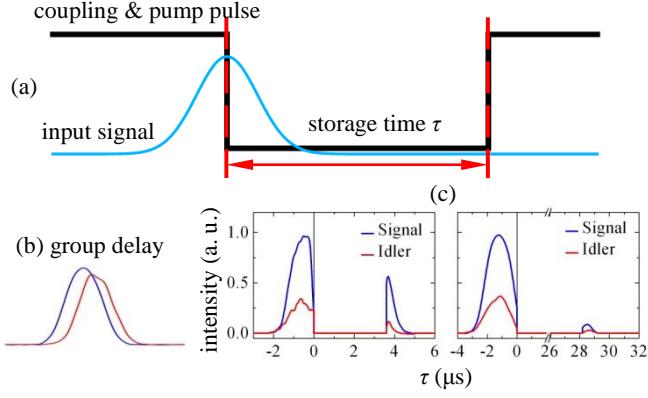


FIG. 2. (a) Representation of the synchronized timing of signal, coupling and pump. (b) Group delay of signal beams in our experiment is about 1μ s. (c) Two experimental results of our FWM storage and retrieval.

The time-dependent interaction Hamiltonian of the three-level Λ system showed in Fig. 1(c) is

$$H_{\text{int}} = -\frac{\hbar}{2} [(\Omega_s e^{i\Delta_s t} + \Omega_p e^{i\Delta_p t})\sigma_{31} + (\Omega_i e^{i\Delta_i t} + \Omega_c e^{i\Delta_c t})\sigma_{32} + \text{H.c.}] \quad (1)$$

where Ω_s , Ω_p , Ω_c , Ω_i denote the Rabi frequencies of signal, pump, coupling, idler fields, Δ_m ($m=s, p, c$ and i) is the detuning of respective fields ($\Delta_s = \omega_{31} - \omega_s$, $\Delta_p = \omega_{31} - \omega_p$, $\Delta_c = \omega_{32} - \omega_c$, $\Delta_i = \omega_{32} - \omega_i$), $\sigma_{ij} = |i\rangle\langle j|$ is atomic projection operator ($i, j=1, 2, 3$), and H.c. stands for Hermitian conjugate. According to energy conservation ($\omega_s + \omega_i = \omega_c + \omega_p$), we have $\Delta_p + \Delta_c = \Delta_s + \Delta_i$. The dynamics of laser-driven atomic system is governed by master equation for the atomic density operator:

$$\frac{d\rho}{dt} = \frac{1}{i\hbar} [H_{\text{int}}, \rho] - D \quad (2)$$

The D is the decoherence matrix

$$D = \begin{pmatrix} -\Gamma_{31}\rho_{33} & \gamma_2\rho_{12}/2 & \gamma_{31}\rho_{13}/2 \\ \gamma_2\rho_{21}/2 & -\Gamma_{32}\rho_{33} & \gamma_{32}\rho_{23}/2 \\ \gamma_{31}\rho_{31}/2 & \gamma_{32}\rho_{32}/2 & \Gamma_3\rho_{33} \end{pmatrix} \quad (3)$$

where Γ_{31} and Γ_{32} are the spontaneous emission rates from state $|3\rangle$ to states $|1\rangle$ and $|2\rangle$, respectively. ρ_{ij} ($i, j=1, 2, 3$) is the element of the density matrix of this system. We have also introduced energy-conserving dephasing processes with rates γ_3 and γ_2 . For convenience, we define the total spontaneous emission rate out of state $|3\rangle$ as $\Gamma_3 = \Gamma_{31} + \Gamma_{32}$. The coherence decay rates are defined as $\gamma_{31} = \Gamma_3 + \gamma_3$, $\gamma_{32} = \Gamma_3 + \gamma_3 + \gamma_2$, and $\gamma_{21} = \gamma_2$. Assuming that $\rho_{11} \approx 1$, $\rho_{22} = \rho_{33} \approx 0$, and $\Omega_c, \Omega_p \gg \Omega_s, \Omega_i$, the steady-state solution for ρ_{12} is

$$\rho_{12} = \frac{\Omega_s \Omega_c^*}{4\Delta_1 \Delta_2 - |\Omega_c|^2} + \frac{\Omega_p \Omega_i^*}{4\Delta_2 \Delta_3 - |\Omega_p|^2} \frac{\Delta_3}{\Delta_1} \quad (4)$$

where we have used a rotating frame to eliminate fast exponential time dependences, and $\Delta_1 = \Delta_s + i\gamma_{31}/2$, $\Delta_2 = \Delta_s - \Delta_c + i\gamma_2/2$ and $\Delta_3 = \Delta_p + i\gamma_{31}/2$ are the complex one-

two- and three-photon detunings, respectively. In our experiment, $\Delta_s = \Delta_c = 0$ MHz, $\Delta_p = \Delta_i = 2\pi \times 80$ MHz, $\gamma_{32} \approx \gamma_{31} = 2\pi \times 3$ MHz and $\gamma_2 = 0.008\gamma_{31}$ [23]. Eq. 6 clearly shows that the signal and idler are coherent in FWM process.

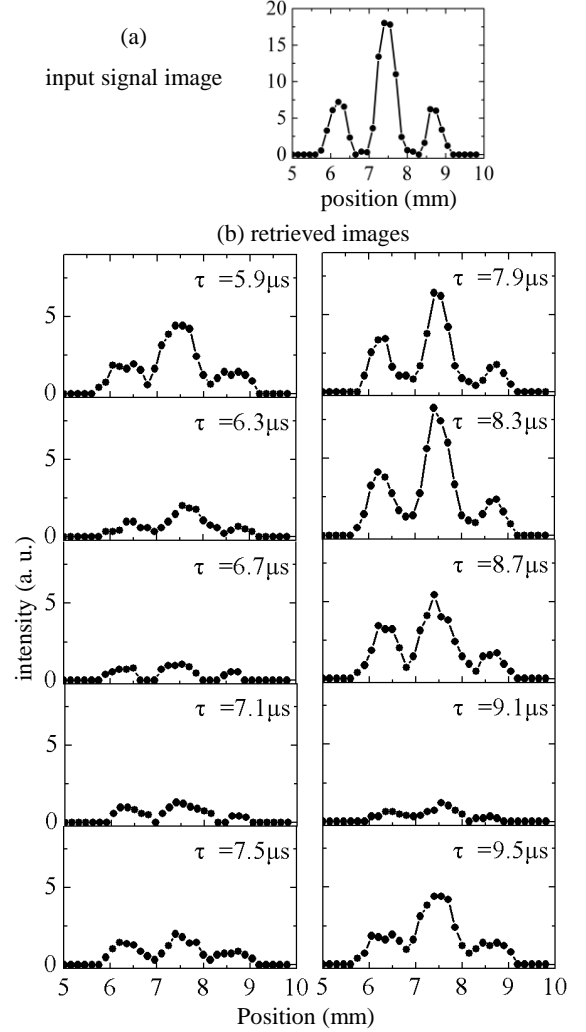


FIG. 3. (a) Input signal profile. (b) The time evolution of retrieved signal fields. We observed the oscillation of retrieved signal versus storage time τ .

The time sequence is showed in Fig. 2(a). Due to the steep dispersion of signal pulse, the group velocity will be greatly reduced (Fig. 2(b)). The delay time in our experiment is about 1μ s (pump is shuttered and coupling is constant), which can efficiently compress the signal pulse in the medium. In Fig. 2(c), we show two FWM storage and retrieval results. The full width at half maximum of the signal pulse is 1.3μ s in our experiment. In the FWM process without storage, the images of signal and idler are shown in Fig. 3(a) and Fig. 4(a), respectively. Here, the images information is extracted by scanning the slit1 in the x -axis and slit2 in the z -axis (Fig. 1(a)). The width of the slits is 0.4 mm. The same method will be used in the extraction of retrieved images. Assuming the

intensities of coupling and pump are constants and they are collimated, the only spatial dependence of idler comes from the signal field amplitude. Due to the phase-matching condition $\mathbf{k}_s + \mathbf{k}_i - \mathbf{k}_c - \mathbf{k}_p = 0$, where \mathbf{k}_s , \mathbf{k}_i , \mathbf{k}_c and \mathbf{k}_p are the wave-vectors of signal, idler, coupling and pump respectively, the generated idler signal will also carry this spatial information.

Assuming the transmission function of the mask is $T(x)=t^2(x)$, and the transverse profile of signal out of fiber is assumed to be Gaussian profile, $I_{s0}\exp(-x^2/d^2)$, where I_{s0} is the peak intensity of signal laser, d is the $1/e^2$ diameter of signal laser, the object's profile is $I_s(x) = T(x) \cdot I_{s0}\exp(-x^2/d^2)$, and the intensity we can get after the slit1 is indicated in Fig. 3(a). Furthermore, the vectorial amplitude of signal is square-root of $I_s(x)$, that is, $\mathbf{E}_s(x) = t(x) \cdot \mathbf{E}_{s0}\exp(-x^2/2d^2)$. At the transform plane, the amplitude of signal $\mathbf{E}_{sf}(\xi)$ is given by the Fourier transform [14]

$$\mathbf{E}_{sf}(\xi) = \mathcal{F}(\mathbf{E}_s) = \frac{1}{\sqrt{\lambda f}} \int_{-\infty}^{\infty} \mathbf{E}_s(x) \exp(-i \frac{2\pi}{\lambda f} x \xi) dx, \quad (5)$$

where ξ is the coordinate of Fourier transform plane, λ the center wavelength of signal and f the focal length of lens L1. The amplitude of idler at the transform plane is $\mathbf{E}_{if}(\xi)$. The spatial pattern and direction of $\mathbf{E}_{if}(\xi)$ are totally determined by the phase-matching condition. The vectorial coherence at the time of storage is given by [17, 18]

$$\rho_{12}(t, \xi) = [g_s \mathbf{E}_{sf} + e^{i\Delta\phi} g_i \mathbf{E}_{if}] \exp((i\omega_{12} - \frac{1}{2\tau})t), \quad (6)$$

where g_s and g_i are the nonlinear coupling coefficients of signal and idler respectively, $\Delta\phi$ is the relative phase between signal and idler, ω_{12} is the splitting of the state $|1\rangle$ and state $|2\rangle$ in an uniform magnetic field, and τ is the decoherence time of this system. The relative phase $\Delta\phi$ is constant [as shown in Fig. 5], which will be discussed below. Here, the diffusion of the atoms is neglected. The uniform magnetic field destroys the degeneracy of the ground state, and the splitting of the Zeeman sublevel cause ρ_{12} evolving likewise with frequency ω_{12} . The time constant τ shows an exponential decay of the energy. As shown in Fig. 2(a), when we adiabatically turn off the coupling and pump, the signal and idler are mapped into the long-lived ground state coherence ρ_{12} . After some time, we turn coupling and pump on, and the ground state coherence (Eq. 6) will be converted back into the electromagnetic fields, *i.e.*, signal and idler. The spatial patterns of retrieved signal and idler are completely determined by the spatial pattern of ρ_{12} (coupling and

pump are assumed to be constants in space) as we see from Eq. 6.

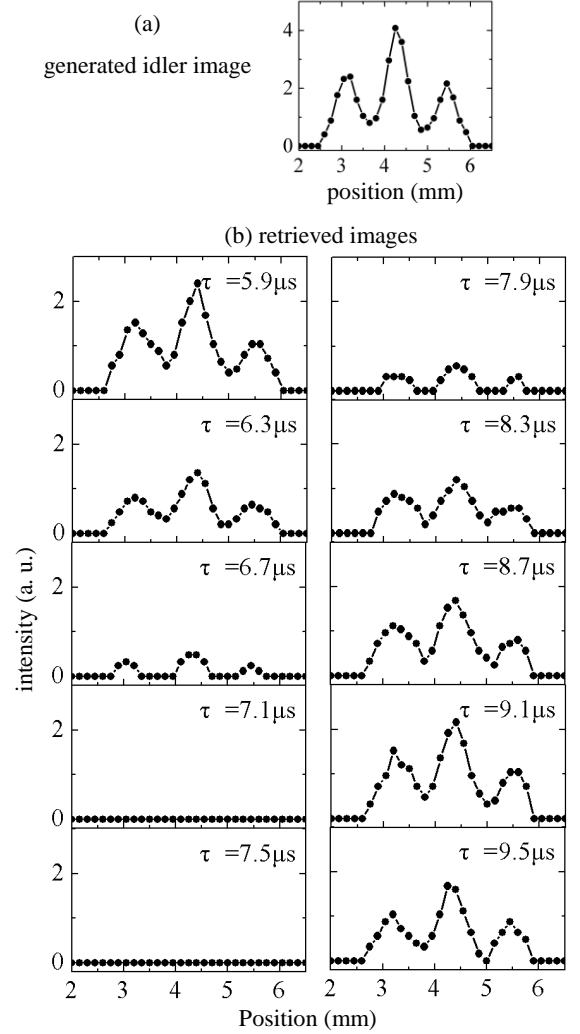


FIG. 4. (a) Generated idler profile. (b) The time evolution of retrieved idler fields. We observed the oscillation of retrieved idler versus storage time τ . The oscillating period is the same to that of signal.

The retrieval efficiencies of signal and idler show some kind of oscillation (Fig. 3(b) and Fig. 4(b)). The phases of the oscillation of the retrieval efficiencies are a little different, which is caused by the erratum of two measurement processes. We have specially studied the oscillation in Fig. 5, where we removed slit1 and slit2 out and detected simultaneously the retrieved intensities of signal and idler directly using PMT1 and PMT2. The oscillation is caused by the Larmor procession of the ground state coherence in the uniform magnetic field [24]. The Larmor period can be expressed as $T_L = 2\pi/\Omega_L$, where $\Omega_L = 2\pi \cdot g_F \mu_B B/h$ is the Larmor frequency, $g_F = 1/3$ is the Landé g -factor for lower ground state $|5^2S_{1/2}, F=3\rangle$, μ_B is the Bohr magneton, B is the magnetic field, and h is Planck constant. In our experiment, the oscillation period is 3.3 μ s and the magnetic field $B=0.65$ G in the z -axis,

which is coincident with the theory. The synchronous retrieval efficiencies may be an implication of the storage of the phases of signal and idler (Eq. 6). The beating between retrieved signal and idler [21] shows the coherence between them is preserved during the storage.

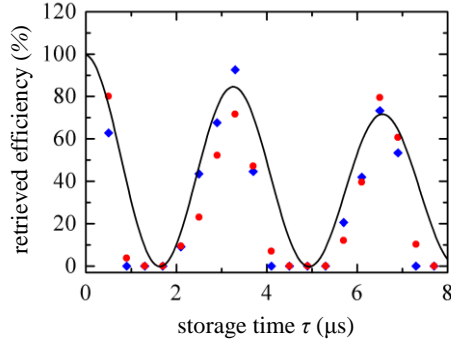


FIG. 5. The oscillation of the retrieval efficiencies of signal (blue diamonds), idler (red circles) and theoretical simulation (black line). The parameters here are period $T_{re}=3.3\mu s$, decoherence time $\tau=20\mu s$, the magnetic field $B=0.16G$ in the z -axis.

In summary, we have showed the storage and retrieval of an image in a cold atomic ensemble using a FWM configuration. The backward-wave geometry and the allowed angle between signal axis and pump axis (that is tolerant in cold atoms) make storage in single-photon level possible. Because of the low temperature of atoms in MOT, the diffusion can be neglected, which enhances the fidelity of this system. Maybe it will find applications in the quantum information processing, remote sensing and image processing.

Acknowledgements

This work was supported by the National Natural Science Foundation of China (Grant Nos. 10874171, 11174271) and the National Fundamental Research Program of China (Grant No. 2011CB00200).

References

- [1] B. Julsgaard, J. Sherson, J. I. Cirac, J. Fiurasek, and E. S. Polzik, *Nature* (London), **432**, 482 (2004).
- [2] C. Liu, Z. Dutton, C. H. Behroozi, and L. V. Hau, *Nature* (London), **409**, 490 (2001).
- [3] D. F. Phillips, A. Fleischhauer, A. Mair, R. L. Walsworth, and M. D. Lukin, *Phys. Rev. Lett.* **86**, 783 (2001).
- [4] N. S. Ginsberg, S. R. Garner, and L. V. Hau, *Nature* (London) **445**, 623 (2007).
- [5] A. V. Turukhin, V. S. Sudarshanam, M. S. Shahriar, J. A. Musser, B. S. Ham, P. R. Hemmer, *Phys. Rev. Lett.* **88**, 023602 (2002).
- [6] L. Allen, M. W. Beijersbergen, R. J. C. Spreeuw, and J. P. Woerdman, *Phys. Rev. A* **45**, 8185 (1992).
- [7] A. Mair, A. Vaziri, G. Weihs, and A. Zeilinger, *Nature* (London), **412**, 313 (2001).
- [8] M. O. O'Sullivan-Hale, I. A. Khan, R. W. Boyd, and J. C. Howell, *Phys. Rev. Lett.* **94**, 220501 (2005).
- [9] M. Jain, A. J. Merriam, A. Kasapi, G. Y. Yin, and S. E. Harris, *Phys. Rev. Lett.* **75**, 4385 (1995).
- [10] R. M. Camacho, C. J. Broadbent, I. A. Khan, and J. C. Howell, *Phys. Rev. Lett.* **98**, 043902 (2007).
- [11] R. Pugatch, M. Shuker, O. Firstenberg, A. Ron, and N. Davidson, *Phys. Rev. Lett.* **98**, 203601 (2007).
- [12] L. Zhao, T. Wang, Y. Xiao, and S. F. Yelin, *Phys. Rev. A* **77**, 041802(R) (2008).
- [13] M. Shuker, O. Firstenberg, R. Pugatch, A. Ben-Kish, A. Ron, and N. Davidson, *Phys. Rev. A* **76**, 023813(2007).
- [14] P. K. Vudiyasetu, R. M. Camacho, and J. C. Howell, *Phys. Rev. Lett.* **100**, 123903 (2008).
- [15] S. E. Harris, *Phys. Today* **50**, No. 7, 36 (1997).
- [16] M. Fleischhauer, A. Imamoglu, and J. P. Marangos, *Rev. Mod. Phys.* **77**, 633 (2005).
- [17] M. Fleischhauer, and M. D. Lukin, *Phys. Rev. Lett.* **84**, 5094 (2000).
- [18] M. Fleischhauer, and M. D. Lukin, *Phys. Rev. A* **65**, 022314 (2002).
- [19] D. A. Braje, V. Balic, S. Goda, G. Y. Lin, and S. E. Harris, *Phys. Rev. Lett.* **93**, 183601 (2004).
- [20] R. M. Camacho, P. K. Vudiyasetu, and J. C. Howell, *Nature Photonics*, **3**, 103 (2009).
- [21] Y. Liu, J.-H. Wu, B.-S. Shi, and G.-C. Guo, "Collapse and revival oscillations of four-wave mixing signal in cold atoms", (submitted).
- [22] M. Fleischhauer, *Nature Photonics*, **3**, 76 (2009).
- [23] Y. Liu, J.-H. Wu, B.-S. Shi, and G.-C. Guo, *Chin. Phys. Lett.* **29**, 024205 (2012).
- [24] D. N. Matsukevich, T. Chanelière, S. D. Jenkins, S.-Y. Lan, T. A. B. Kennedy, and A. Kuzmich, *Phys. Rev. Lett.* **96**, 033601 (2006).